*JID*Open

Potent Dual Inhibitors of TORC1 and TORC2 Complexes (KU-0063794 and KU-0068650) Demonstrate *In Vitro* and *Ex Vivo* Anti-Keloid Scar Activity

Farhatullah Syed[1,2], Hitesh J. Sanganee[3], Ashwani Bahl[3] and Ardeshir Bayat[1,2,4]

Mammalian target of rapamycin (mTOR) is essential in controlling several cellular functions. This pathway is dysregulated in keloid disease (KD). KD is a common fibroproliferative dermal lesion with an ill-defined treatment strategy. KD demonstrates excessive matrix deposition, angiogenesis, and inflammatory cell infiltration. In KD, both total and phosphorylated forms of mTOR and $p70^{S6K}$(Thr421/Ser424) are upregulated. Therefore, the aim of this study was to investigate adenosine triphosphate–competitive inhibitors of mTOR kinase previously unreported in keloid and their comparative efficacy with Rapamycin. Here, we present two mTOR kinase inhibitors, KU-0063794 and KU-0068650, that target both mTORC1 and mTORC2 signaling. Treatment with either KU-0063794 or KU-0068650 resulted in complete suppression of Akt, mTORC1, and mTORC2, and inhibition of keloid cell spreading, proliferation, migration, and invasive properties at a very low concentration ($2.5\,\mu mol\,l^{-1}$). Both KU-0063794 and KU-0068650 significantly ($P<0.05$) inhibited cell cycle regulation and HIF1-α expression compared with that achieved with Rapamycin alone. In addition, both compounds induced shrinkage and growth arrest in KD, associated with the inhibition of angiogenesis, induction of apoptosis, and reduction in keloid phenotype–associated markers. In contrast, Rapamycin induced minimal antitumor activity. In conclusion, potent dual mTORC1 and mTORC2 inhibitors display therapeutic potential for the treatment of KD.

INTRODUCTION

The mammalian target of Rapamycin (mTOR) is a 289-kDa serine–threonine kinase that regulates cellular activity (Dazert and Hall, 2011). mTOR kinases form two distinct multiprotein complexes mTORC1 and mTORC2. Inhibition of mTORC1 alone by rapalogs leads to enhanced activation of PI3K axis by the mTOR-S6K-IRS1-negative feedback loop (Bracho-Valdes

et al., 2011). mTORC2 phosphorylates Akt on Ser473, increasing its enzyme activity up to 10-fold (Chresta *et al.*, 2010). Activated Akt regulates many cellular functions. Thus, mTORC2 is an attractive target in cancer (Sini *et al.*, 2010; Sparks and Guertin, 2010).

Keloid disease (KD) is a fibroproliferative lesion characterized by excessive deposition of extracellular matrix (ECM) such as collagen (Shih *et al.*, 2010), fibronectin (FN), and α-smooth muscle actin (α-SMA) (Supplementary Figure S1a online) (Ong *et al.*, 2007). KD fibroblasts possess cancer-like properties (Vincent *et al.*, 2007), with overexpression of cytokines and increased angiogenesis (Shih *et al.*, 2010) (Supplementary Figure S1b online). KD infiltrates the surrounding tissue with up to 80% recurrence post excision (Mall *et al.*, 2002). Many treatment modalities exist, but they fail to prevent KD recurrence (Patel and Lawrence Cervino, 2010), hence the urgency for effective treatment options. mTOR is a regulator of collagen expression in dermal fibroblasts shown by the inhibition of ECM deposition with Rapamycin (Shegogue and Trojanowska, 2004). The PI3K/Akt/mTOR pathway leads to the overproduction of ECM in KD, and targeting of the mTOR pathway is a potential therapeutic approach in eradicating keloids (Lim *et al.*, 2003; Zhang *et al.*, 2006; Ong *et al.*, 2007). We hypothesized that dual mTORC1

[1]Plastic & Reconstructive Surgery Research, Manchester Institute of Biotechnology, University of Manchester, Manchester, UK; [2]Faculty of Medical and Human Sciences, Manchester Academic Health Science Centre, University Hospital of South Manchester NHS Foundation Trust, Institute of Inflammation and Repair, University of Manchester, Manchester, UK; [3]New Opportunities iMed, AstraZeneca R&D Alderley Park, Macclesfield, Cheshire, UK and [4]Manchester Academic Health Science Centre, University of Manchester, Manchester, UK

Correspondence: Ardeshir Bayat, Plastic & Reconstructive Surgery Research, Manchester Institute of Biotechnology, University of Manchester, 131 Princess Street, Manchester M1 7DN, UK. E-mail: Ardeshir.Bayat@manchester.ac.uk

Abbreviations: α-SMA, α-smooth muscle actin; AZ, AstraZeneca; ECM, extracellular matrix; ELF, extra-lesional fibroblast; ELT, extra-lesional tissue; FN, fibronectin; KD, keloid disease; KF, keloid fibroblast; mTOR, mammalian target of rapamycin; OC, organ culture; RTCA, real-time cell analysis; WST-1, water-soluble tetrazolium salt-1

and mTORC2 inhibition provides superior inhibition of Akt signaling and anti-angiogenic activity. Unlike Rapamycin, which inhibits mTORC1 alone (Benjamin *et al.*, 2011), here we demonstrate that both KU-0063794 and KU-0068650 (referred to collectively as AstraZeneca (AZ) compounds) are highly selective adenosine triphosphate-competitive inhibitors (Garcia-Martinez *et al.*, 2009) of mTOR kinase activity, with no toxicity *in vivo* (Malagu *et al.*, 2009; Janes *et al.*, 2010; Dormond-Meuwly *et al.*, 2011), similar in mechanism of action to AZD8055 (Chresta *et al.*, 2010; Sini *et al.*, 2010).

Therefore, we investigated (i) the baseline cellular levels of mTOR, p70S6K, and their activated forms between KD and extra-lesional tissue (ELT) obtained from the same patient, (ii) the effect of both AZ compounds on KD growth and ECM deposition *in vitro* and *ex vivo*, and (iii) differences between KU-0063794 and KU-0068650 to a well-recognized mTOR inhibitor Rapamycin.

RESULTS
Overexpression of Total and Phosphorylated forms of mTOR and $p70^{S6K}$
There was a differential expression of mTOR and $p70^{S6K}$ and their phosphorylated forms in KD compared with ELT and extra-lesional fibroblasts (ELFs) (Supplementary Figure S1c online). Total and phosphorylated forms of mTOR showed high expression of both forms in KD compared with ELT (Figure 1a). The average total immunoreactivity using In-Cell Western Blotting showed a significant (*$P<0.02$) increase in mTOR, p-mTOR, $p70^{S6K}$, and phospho-$p70^{S6K}$(Thr421/Ser424) in keloid fibroblasts (KFs) compared with ELFs (Figure 1b and c). Thus, mTOR is active in KD.

Concentration-dependent effect of KU-0063794 and KU-0068650 on PI3K/AKT/mTOR intracellular signaling
The inhibitory potential of both AZ compounds was compared with Rapamycin, an allosteric mTORC1 inhibitor (Benjamin *et al.*, 2011), in intracellular PI3K/Akt/mTOR signaling of KFs and ELFs. Both AZ compounds demonstrated a dose-dependent, significant ($P<0.01$) decrease in pAkt-S473. mTORC1 downstream substrates, 4E-BP1, and S6 ribosomal protein were efficiently ($P<0.01$) dephosphorylated. Both AZ compounds neither inhibited phosphorylated mitogen-activated protein kinase nor pAkt-T308 at a low concentration ($2.5\,\mu mol\,l^{-1}$). Furthermore, both AZ compounds reduced ($P<0.05$) phosphorylation of GSK3β, a critical downstream element of the PI3kinase/Akt and HIF1-α ($P<0.01$). Rapamycin ($20\,\mu mol\,l^{-1}$) significantly reduced pAkt-T308, but had no effect on pAkt-S473 (Figure 1d). Both AZ compounds did not cause inhibition of PI3K/Akt/mTOR signaling in ELFs at $2.5\,\mu mol\,l^{-1}$ (Supplementary Figure S2 online). This discrepancy could be due to reduced expression of mTOR and p-mTOR in ELFs compared with KFs. Therefore, both AZ compounds appear specific in the inhibition of pAkt-S473.

Dissociation of mTORC1 and mTORC2 complexes by KU-0063794 and KU-0068650
Both AZ compounds showed a significant ($P\leqslant0.01$) reduction of p-mTOR, Rictor, and Raptor immunoreactivity (Figure 1e).

In contrast, Rapamycin only reduced p-mTOR and Raptor immunoreactivity ($P<0.05$). To confirm the effect on the mTORC1 and mTORC2 complex observed in KFs, we performed an immunoprecipitation assay. Predictably, both AZ compounds inhibited the association of mTORC1 with Raptor and mTORC2 with Rictor, whereas Rapamycin failed to show mTORC2 inhibition in KFs (Figure 1f). These results demonstrate that both AZ compounds inhibit mTORC1 and mTORC2 inhibitors as described previously with AZD8055 (Chresta *et al.*, 2010) and P529 (Xue *et al.*, 2008).

KU-0063794 and KU-0068650 reduced viability/metabolic activity and inhibited cell spreading, attachment, and proliferation in a concentration-dependent manner
The effect of KU-0063794 and KU-0068650 on cell behavior was compared with Rapamycin with the water-soluble tetra-zolium salt-1 (WST-1) assay using a range of concentrations. Treatment with different concentrations resulted in significant ($P\leqslant0.03$) reduction in cell viability/metabolic activity in a dose-dependent manner. However, both AZ compounds had a significantly ($P<0.03$) higher effect on KFs compared with ELFs. In contrast, Rapamycin showed a similar effect on KFs and ELFs. After compound removal, the effect of Rapamycin recovered in both KFs (Figure 2a) and ELFs (Figure 2b) compared with both AZ compounds.

The cell growth inhibition displayed by both AZ compounds was evaluated using a label-free real-time cell analysis (RTCA) on a microelectronic sensor array (Syed *et al.*, 2012a,b). Both AZ compounds ($P<0.02$) and Rapamycin significantly ($P<0.05$) inhibited cell spreading, attachment, and proliferation in a time- and dose-dependent manner in KFs. Similar dose-dependent and time-dependent inhibitions were also seen in ELFs. In addition, both AZ compounds had a sustained effect on KFs and ELFs seen by the recovery of cells after removal of the inhibitors at 24 hours. When treatment with all three compounds was complete, KFs and ELFs were not able to recover within 26–30 hours compared with the vehicle-treated group. Importantly, in the KU-0068650-treated group, the average cell index was reduced further, suggesting that the effect was sustained in this group. However, in the KU-0063794- and Rapamycin-treated groups, there was an increase in the average cell index in KFs (Figure 2c and Supplementary Figure S3a online) compared with ELFs (Supplementary Figure S3b and c online). Compared with Rapamycin ($20\,\mu mol\,l^{-1}$), KU-0063794 and KU-0068650 were highly effective even at a very low concentration ($2.5\,\mu mol\,l^{-1}$). Taken together, both AZ compounds significantly ($P<0.05$) decreased KF and ELF proliferation in a concentration- and time-dependent manner.

KU-0063794 and KU-0068650 strongly inhibited the migration and invasion properties of KFs and induced apoptosis in a concentration-dependent manner
Cell growth inhibition properties of both AZ compounds were evaluated using an *in vitro* collagen-coated two-dimensional migration assay. Treatment with both AZ compounds significantly ($P<0.01$) reduced the migration of KFs compared with the Rapamycin-treated group, in a concentration-dependent
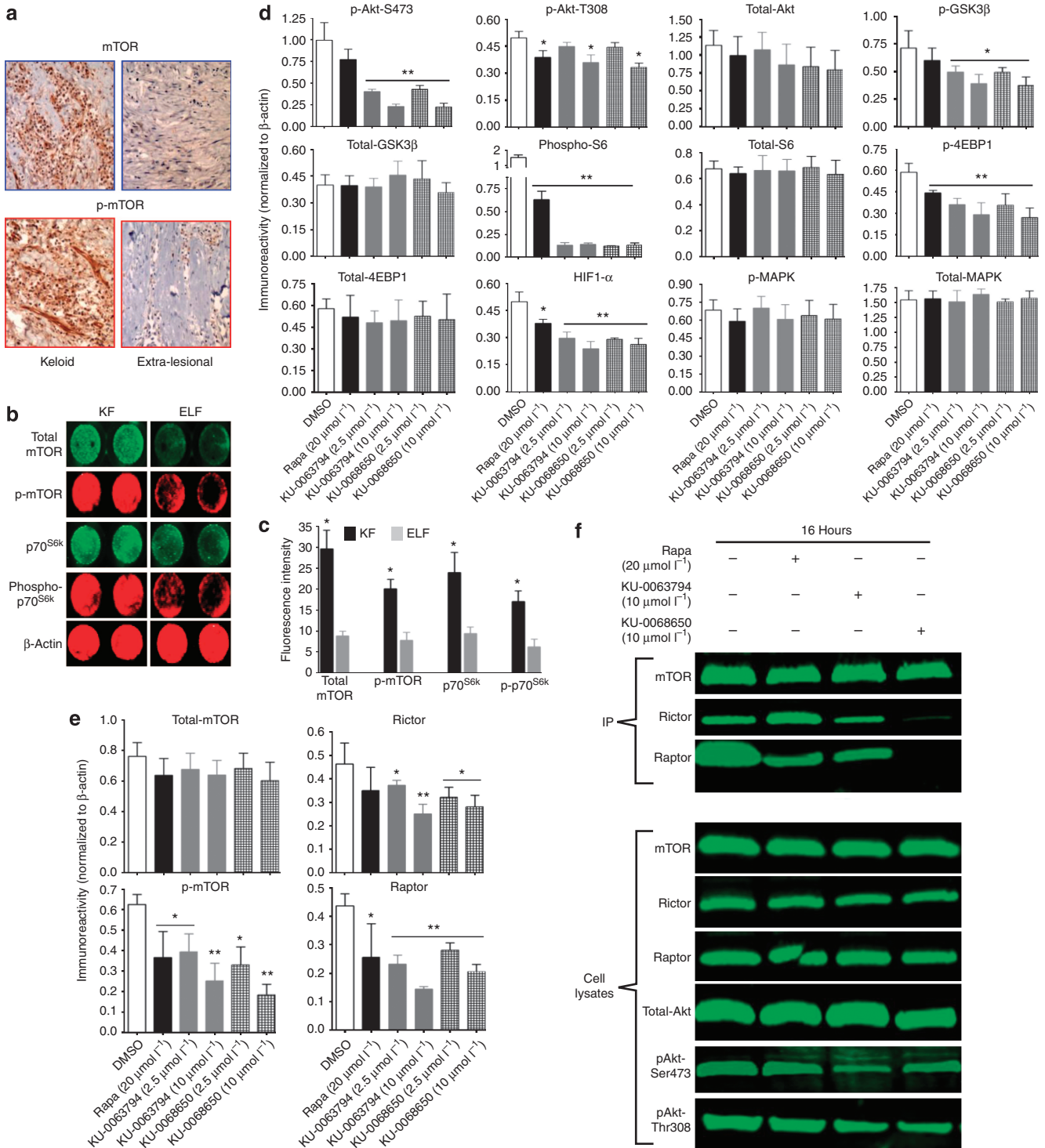
Figure 1. Inhibition of intracellular signaling in keloid fibroblast (KF) by both KU-0063794 and KU-0068650. (**a**) Differential expression of mammalian target of rapamycin (mTOR) and phosphor-mTOR (p-mTOR) ($n=6$). (**b**) Differential expression of mTOR signaling in KFs and extra-lesional fibroblasts (ELFs) using In-Cell Western Blotting (ICWB) ($n=11$). (**c**) ICWB average immunoreactivity from (**b**). (**d**) ICWB average immunoreactivity of KF ($n=11$) induced mTOR inhibitors, normalized to β-actin. (**e**) Both KU-0063794 and KU-0068650 inhibit mTORC1 and mTORC2 in primary KFs. Bar graphs represent the quantification of average protein expression in different treatments from three independent ICWB experiments ($n=6$). (**f**) Co-immunoprecipitation for mTOR with raptor and Rictor to assess TORC1 and TORC2 complex inhibition by both the compounds ($n=11$). The data presented here are the means ± SEM of triplicate experiments performed. **$P<0.05$, *$P\leqslant0.01$ indicate significant difference in the treated group compared with the DMSO control group. AKT, also known as protein kinase B (PKB); 4E-BP1, eukaryotic initiation factor 4 E-binding protein-1; GSK3β, glycogen synthase kinase-3; HIF-1α, hypoxia-inducible factor-1alpha; IP, immunoprecipitation; MAPK, mitogen-activated protein kinase; p-MAPK, phosphorylated mitogen-activated protein kinase; Raptor, regulatory associated protein of mTOR; Rictor, rapamycin-insensitive companion of mTOR.
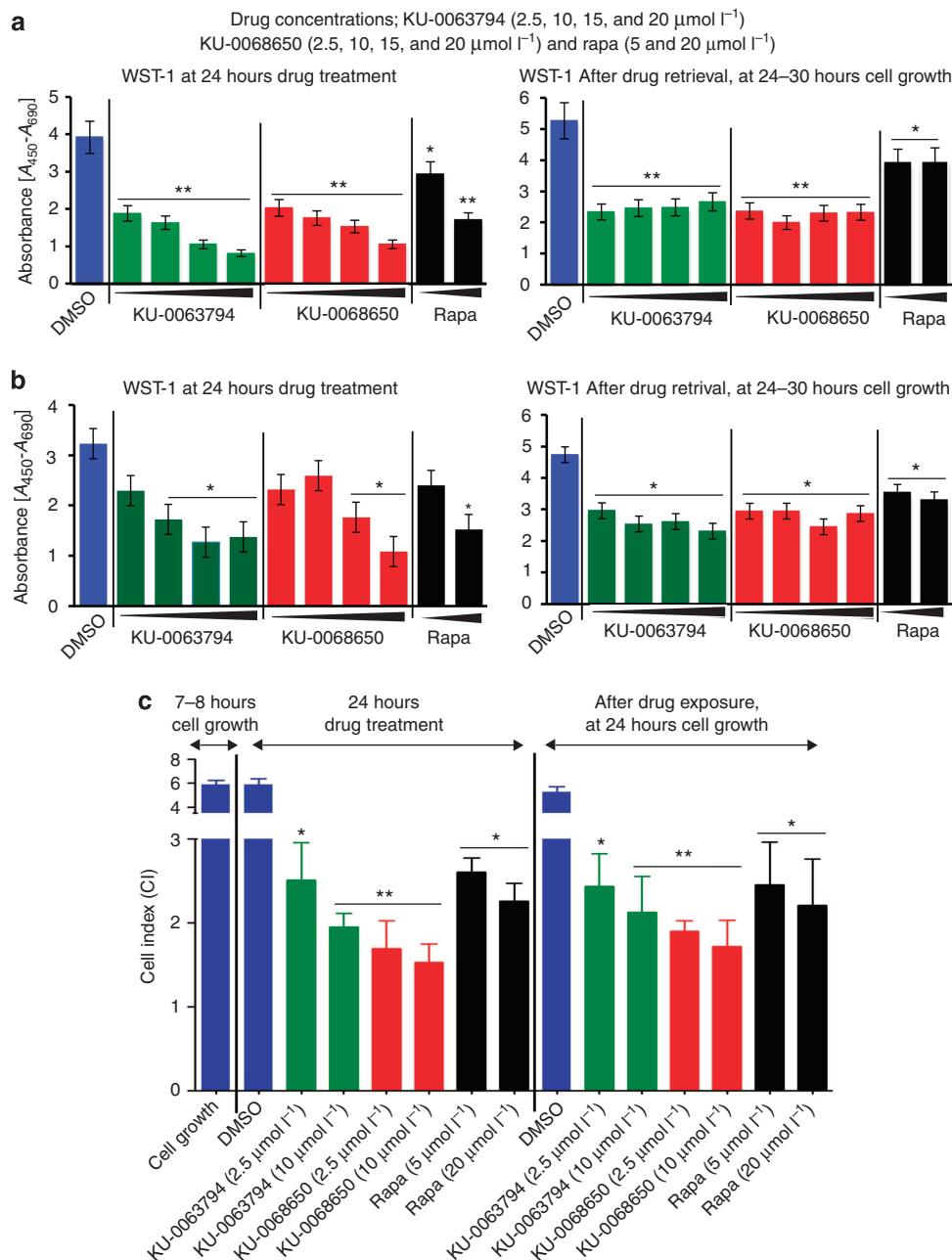
Figure 2. **Role of mammalian target of rapamycin (mTOR) inhibitors on keloid cell viability/metabolic activity by water-soluble tetrazolium salt-1 (WST-1), cell adhesion, spreading, and proliferation by real-time cell analysis (RTCA) on microelectronic sensor arrays.** (**a**) WST-1 assay was performed 24 hours post treatment with different mTOR inhibitors, for viability/metabolic activity (keloid fibroblast (KF): $n = 8$). (**b**) WST-1 assay for extra-lesional fibroblasts ($n = 5$). (**c**) Quantitative analysis of RTCA average cell index of KFs ($n = 9$). Primary KFs were seeded on 96-well E-plate (1×10^4 cells per well) and cells were treated with different mTOR inhibitor concentrations. Cell index (CI) on RTCA was recorded every 15 minutes. **P < 0.04, *P ≤ 0.01 indicate significant difference compared with the DMSO control group. The data expressed are an average means ± SEM from four independent experiments.

manner. Rapamycin also reduced the migration of KFs significantly ($P < 0.05$), but at a higher concentration ($20 \mu mol\, l^{-1}$) compared with the vehicle control. However, migration inhibitory effect by both AZ compounds was low in ELFs compared with KFs (Figure 3a and b).

An Oris three-dimensional basement membrane extract invasion and detection assay was used to assess the anti-invasive properties of both AZ compounds. KFs showed a high

level of invasion ($P < 0.01$) compared with ELFs. Treatment with both AZ compounds significantly ($P < 0.01$) reduced the invasive properties of KFs at 48 hours post treatment, whereas Rapamycin showed significant ($P < 0.05$) inhibition of KF invasion with a low efficacy compared with both AZ compounds (Figure 3c and d). These results suggest that both AZ inhibitors have potential anti-invasive properties.
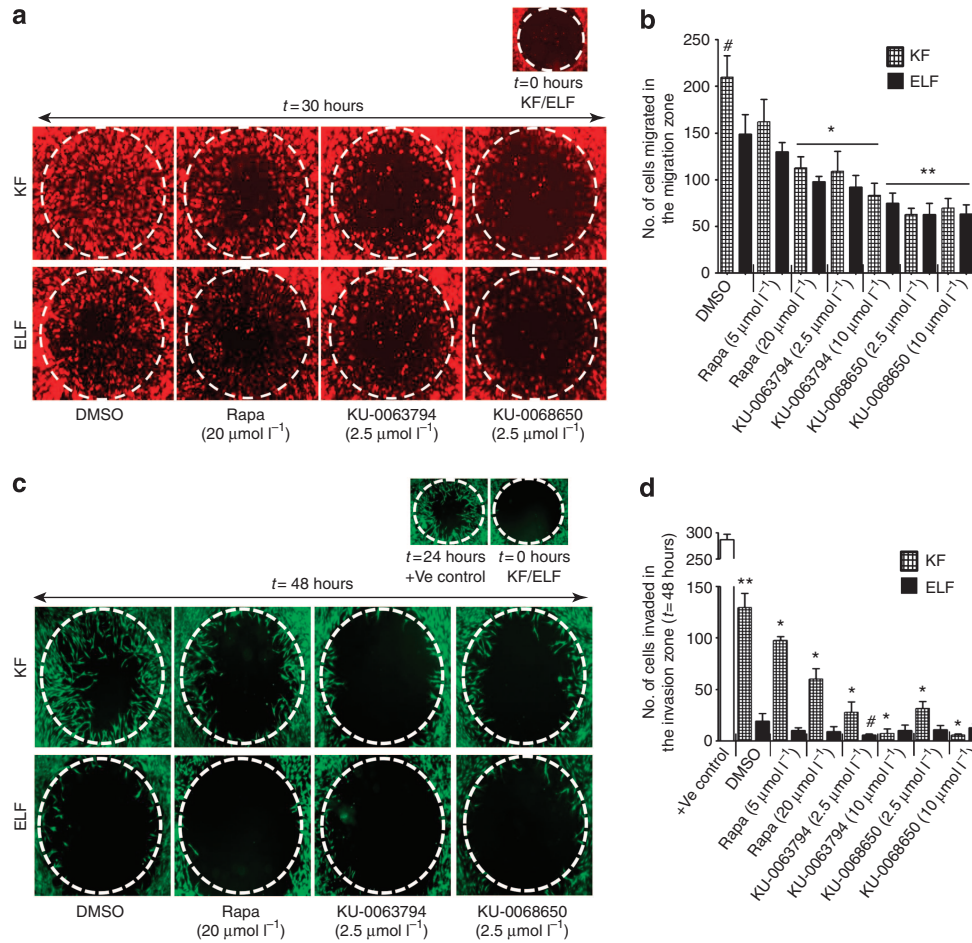
Figure 3. Differential effect of KU-0063794, KU-0068650, and Rapamycin on primary keloid fibroblast (KF) and extra-lesional fibroblast (ELF) migration and invasion properties. (**a**) Fibroblast migration response toward the 2-mm migration zone, in an *in vitro* two-dimensional collagen assay. Representative micrographs are shown from three independent experiments. (**b**) The average number of migrated fibroblasts in the migration zone with and without compounds. *$P < 0.05$, significant difference compared with the DMSO group. **$P \leqslant 0.01$, significant difference compared with the Rapamycin group. #$P < 0.05$, significant difference in KF migration compared with ELFs. (**c**) Fibroblasts' invasive response toward the 2-mm invasion zone in an *in vitro* three-dimensional basement membrane extract model. (**d**) The average number of invaded cells in the invasion zone. **$P < 0.01$ indicates significant difference compared with primary ELFs. *$P < 0.03$ indicates significant difference in primary KFs compared with the DMSO group. #$P < 0.05$ indicates significant difference in primary ELFs compared with the DMSO group.

On the basis of the WST-1 and RTCA results, it was hypothesized that both AZ compounds may achieve their inhibitory effect via apoptosis or cellular necrosis. Indeed, both compounds induced significant apoptosis, as there was an increase in Annexin V–positive cells ($P < 0.05$) at 24 hours post treatment, compared with Rapamycin ($5 \mu mol \, l^{-1}$) and control group, in a concentration-dependent manner. However, higher doses ($20 \mu mol \, l^{-1}$) of Rapamycin also caused significant ($P < 0.05$) apoptosis. Importantly, both AZ compounds caused a reduced level of apoptosis in ELFs compared with KFs (Supplementary Figure S4a and b online). Thus, both AZ compounds inhibited cellular activity by inducing apoptosis.

KU-0063794 and KU-0068650 downregulated ECM, cell cycle markers, and decreased fibroblast proliferation in a concentration-dependent manner
Both KU-0063794 and KU-0068650 significantly ($P \leqslant 0.01$) downregulated the expression of collagen, FN, and α-SMA

compared with Rapamycin ($P \leqslant 0.05$) in a concentration-dependent manner at messenger RNA in KFs (Figure 4a) and protein levels in both KFs (Figure 4b and Supplementary Figure S5a–c online) and ELFs (Supplementary Figure S5a–d online). However, both AZ compounds inhibited ECM-related proteins in ELFs, at higher concentrations compared with KFs.

RTCA and WST-1 analyses demonstrated reduced levels of cell proliferation and viability/metabolic activity. The expression levels of cell cycle proteins proliferating cell nuclear antigen and Cyclin D were significant. Concentration-dependent downregulation was observed in fibroblasts treated with both AZ compounds at protein levels. However, Rapamycin showed a significant ($P < 0.05$) reduction in proliferating cell nuclear antigen and Cyclin D expression at a higher concentration compared with vehicle control (DMSO) in KFs and ELFs. Both AZ compounds had a minimal effect on cell cycle proteins at $2.5 \mu mol \, l^{-1}$ in ELFs (Figure 4b and Supplementary Figure S5d online).
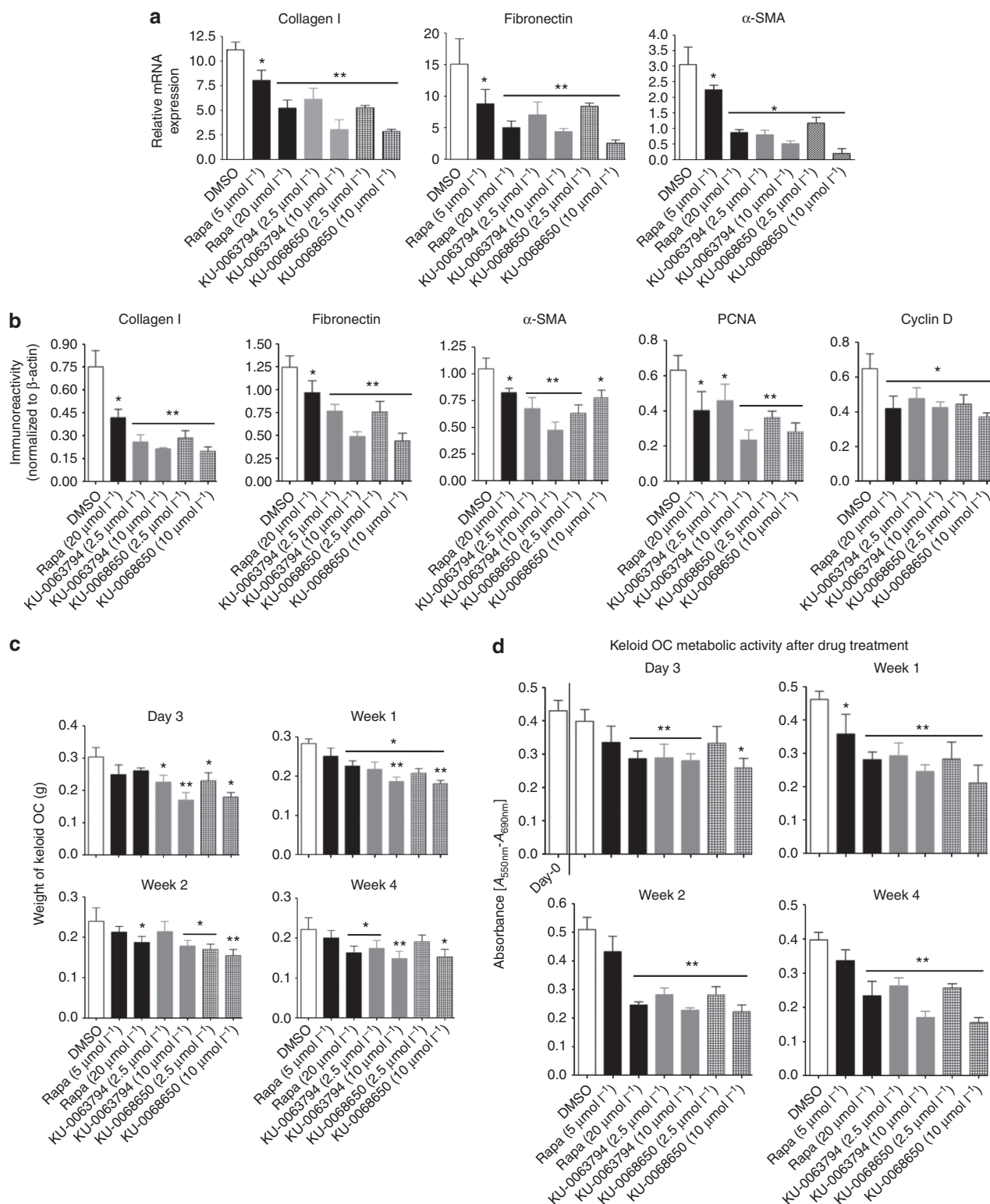
Figure 4. Effect of KU-0063794 and KU-0068650 compounds compared to Rapamycin in *in vitro* and *ex vivo* keloid models. (**a**) Both KU-0063794 and KU-0068650 inhibit the expression of collagen, fibronectin, and α-smooth muscle actin (α-SMA) at messenger RNA (mRNA) levels (keloid fibroblast (KF): $n = 8$). (**b**) In-Cell Western Blotting analysis of the expression of ECM proteins, Cyclin D, and proliferating cell nuclear antigen (PCNA), 24 hours post treatment with different mammalian target of rapamycin inhibitors (KF: $n = 8$). (**c**) Shrinkage of keloid organ culture (OC) after different compound treatments. Average weight of the keloid OC ($n = 10$) at different time points are indicated in the bar graph. Four millimeter keloid explant biopsies were removed from the collagen gel matrix and its weight was determined in triplicates. (**d**) In MTT 3-(4,5-dimethylthiazol-2-yl)-2,5-diphenyltetrazolium bromide assay both, KU-0063794 and KU-0068650 showed much greater inhibitory effect on metabolic activity in keloid OC ($n = 8$) as compared with Rapamycin. $*P < 0.05$, $**P \leqslant 0.01$ indicates significant difference compared with the DMSO group.

KU-0063794 and KU-0068650 induced apoptosis and significantly reduced keloid volume and metabolic activity in an *ex vivo* model

To evaluate the therapeutic potential of both AZ compounds in KD, we used an *ex vivo* keloid organ culture (OC) model (Bagabir *et al.*, 2012) as described previously. Both AZ compounds ($10 \mu mol\,l^{-1}$) significantly ($P \leqslant 0.02$) induced the shrinkage and reduced the keloid OC volume compared with the vehicle group on day 3. However, Rapamycin treatment ($20 \mu mol\,l^{-1}$) also significantly ($P < 0.05$) decreased the average weight of the keloid OC at week 1 compared with the vehicle group (Figure 4c and Supplementary Figure S6a online).

Both AZ compounds ($2.5 \mu mol\,l^{-1}$) and Rapamycin significantly ($P < 0.05$) reduced metabolic activity from day 3 to week 4 as compared with the vehicle group evidenced by an MTT 3-(4,5-dimethylthiazol-2-yl)-2,5-diphenyltetrazolium bromide assay (Figure 4d). Furthermore, both AZ compounds significantly ($P < 0.02$) increased apoptosis on day 3 *in situ* compared with the Rapamycin-treated group. However, Rapamycin did not cause any significant apoptosis until week 1 post treatment, compared with the vehicle group. At week 4, 55–65% TUNEL-positive cells were observed in both the AZ inhibitor ($10 \mu mol\,l^{-1}$)–treated groups, whereas the Rapamycin ($20 \mu mol\,l^{-1}$)-treated group showed only 35–40% TUNEL-positive cells (Figure 5a and b). Thus, both AZ compounds caused shrinkage of keloid tissue in an *ex vivo* model on day 3 post treatment, plus they reduced metabolic activity and induced massive apoptosis at $2.5 \mu mol\,l^{-1}$ compared with Rapamycin ($20 \mu mol\,l^{-1}$) in a keloid *ex vivo* model.

Tissue morphological analysis revealed reduced cellularity/inflammation and angiogenesis by KU-0063794 and KU-0068650

In hematoxylin and eosin–stained tissue sections, histological changes were evaluated in the epidermis, papillary dermis, and reticular dermis. Up to day 3, the overall tissue architecture was well preserved in the Rapamycin-treated group, whereas at week 1 both AZ compound–treated groups showed reduced cellularity and thinning of the stratum granulosum and papillary dermis. Both KU-0063794- and KU-0068650-treated groups showed that the epidermis was completely detached from week 1 to week 4 of treatment and exhibited more intense tissue damage, characterized by keloid cell loss, increased number of cells with pyknotic nuclei, and reduced fibrosis (thick collagen bundles). In contrast, Rapamycin showed minimal effect on keloid OC despite a higher concentration ($20 \mu mol\,l^{-1}$). However, at week 4, Rapamycin-treated explants showed detachment of the epidermis, with increased number of cells showing pyknotic nuclei, although the overall structure was better preserved compared with AZ compound–treated keloid tissue. Both AZ compounds also induced a noticeable decrease in the hyalinized collagen bundles in the keloid tissue model at week 1 through to week 4 (Supplementary Figure S6b online).

Keloid tissue shows increased blood vessel density compared with extra-lesional skin (Supplementary Figure S1b online). Therefore, we examined the anti-angiogenic and anti-vascular properties of both AZ compounds. Indeed, these showed a drastic reduction in the number of CD31 + ve (endothelial cell marker) (Figure 5c) and CD34 + ve (a microvascular endothelial cell marker) cells (Figure 5d) in the papillary and reticular dermis at week 1 up to week 4. In contrast, Rapamycin showed a noticeable reduction in both anti-CD31 and anti-CD34 expression only at week 4. The above findings suggest that significant shrinkage of keloid tissue in both AZ compound–treated groups may be due to a combination of anti-proliferative and apoptotic effects along with a compound-related anti-angiogenic and anti-vascular effect.

Inhibition of PI3K-Akt-mTOR signaling in keloid OC model by KU-0063794 and KU-0068650

To evaluate the *ex vivo* effects of both AZ compounds compared with Rapamycin, on intracellular signaling *in situ*, tissue was analyzed with immunohistochemistry post treatment. In both KU-0063794- and KU-0068650-treated groups, the expression of pAkt-S473 (Supplementary Figure S7a online), p-mTOR (Supplementary Figure S7b online), and pS6 (Supplementary Figure S7c online) was reduced at week 1 compared with the Rapamycin-treated group, whereas in the Rapamycin-treated group pAkt-S473, p-mTOR, and pS6 reduced at week 4.

KU-0063794 and KU-0068650 suppressed pro-collagen, FN biosynthesis, and α-SMA expression in the keloid OC model

Finally, we elucidated the potential anti-fibrotic effect of both KU-0063794 and KU-0068650 in keloid OC *in situ*. As expected, treatment with both AZ inhibitors reduced the immunoreactivity of pro-collagen I at week 1 post treatment compared with the Rapamycin-treated group (Supplementary Figure S8 online). Similarly, FN was reduced by both AZ compounds on day 3 and week 1 compared with the Rapamycin-treated group (Supplementary Figure S9a online). We also assessed for the expression of α-SMA, which showed a significant reduction by both the AZ compounds at week 1 up to week 4 (Supplementary Figure S9b online). Nevertheless, Rapamycin also suppressed the expression level of pro-collagen, FN, and α-SMA at week 1 up to week 4 at a higher concentration compared with the vehicle group. In summary, both AZ compounds caused a significant reduction of ECM-related proteins in keloid tissue compared with Rapamycin.

DISCUSSION

Using *in vitro* and *ex vivo* experiments, here we demonstrate two compounds, previously unreported in keloid, KU-0063794 and KU-0068650, that show promising anti-fibrotic activity. Both compounds are not only potent but also selective mTORC1 and mTORC2 inhibitors compared with Rapamycin.

Both AZ compounds attenuated Akt phosphorylation at specific Ser473 and significantly inhibited mTORC1 and mTORC2 complexes, whereas Rapamycin only inhibited the mTORC1 complex. Consistent with our results, recently, KU-0063794 (Garcia-Martinez *et al.*, 2009), AZD8055 (Chresta
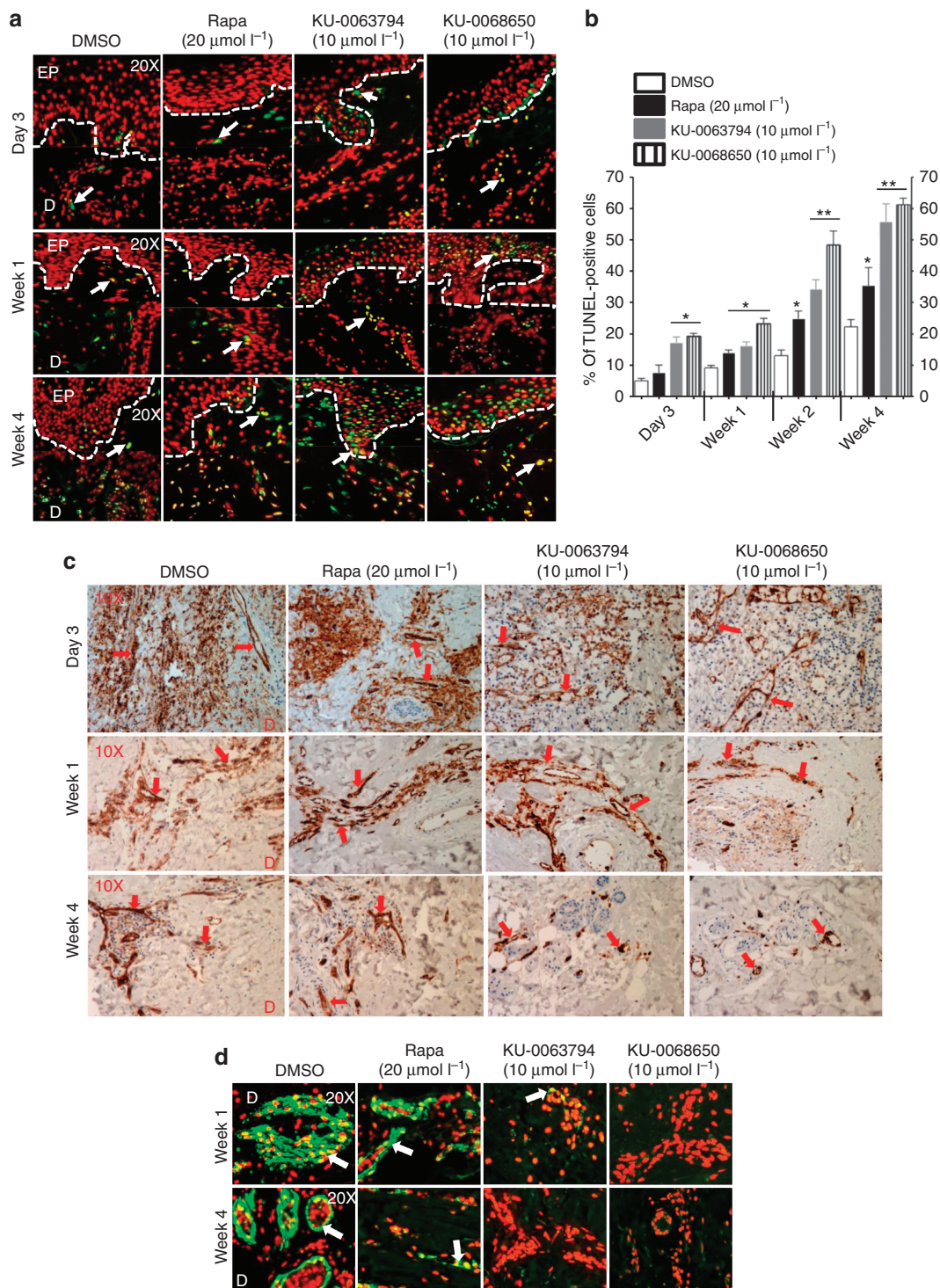
Figure 5. Both KU-0063794 and KU-0068650 compounds induce apoptosis and deplete CD31 and CD34 + Ve cells in keloid organ culture. (**a**) Representative micrographs of TUNEL staining (red-nuclei and green–yellow TUNEL + Ve cells) (*n* = 8). Original magnification, × 200. D, dermis; EP, epidermis. Arrows indicate TUNEL + Ve cells. (**b**) % of TUNEL + Ve cells (*n* = 8). *P < 0.05, **P < 0.01 indicates significant difference compared with the DMSO control group. (**c**) Representative micrographs of CD31 + Ve endothelial cells after different compound treatments (*n* = 8). Original magnification × 100. Arrows indicate CD31 + Ve cells. (**d**) Representative micrographs of CD34 + Ve microvascular endothelial cell marker after different compound treatments. Original magnification, × 200. Red, nuclei; green, CD34 + Ve cells. Arrows indicate CD34 + Ve cells.

et al., 2010; Marshall *et al.*, 2011), Palomid 529 (Xue *et al.*, 2008), NVP-BEZ235 (Chapuis *et al.*, 2010; Santiskulvong *et al.*, 2011), and WYE-125132 (Yu *et al.*, 2010) have shown

similar inhibitory effect on mTORC1 and mTORC2. These results demonstrate that these AZ compounds have a potential anti-fibrotic effect. Both AZ compounds showed more

effective inhibition of KF cell attachment, spreading, proliferation, and caused cytotoxicity and reduced viability/metabolic activity, as well as inhibited migration and invasion properties at a low concentration ($2.5\,\mu mol\,l^{-1}$) compared with Rapamycin ($20\,\mu mol\,l^{-1}$).

The cell inhibition properties were achieved partly by suppressing proliferating cell nuclear antigen and cyclin D. Reorganization of the actin cytoskeleton is a multistep process and is an early event in cellular activity (Bracho-Valdes *et al.*, 2011). Both AZ compounds are potent inhibitors of mTORC2 (Jacinto *et al.*, 2004; Bracho-Valdes *et al.*, 2011), and this may explain the inhibition of keloid cell attachment, spreading, migration, and invasion. In the initial *in vitro* experiments, using lactate dehydrogenase (cytotoxicity) assay, both AZ compounds showed toxicity in keloid and ELFs. However, the efficacy of both compounds was reduced in ELFs. Importantly, the effect of both compounds was reversible within 24 hours of drug removal in extra-lesional primary fibroblasts but not in KFs (data not shown). From these results, both AZ compounds are highly selective in inhibiting KF activity.

Activation of the PI3K/Akt/mTOR pathway is important for cell growth (Morgensztern and McLeod, 2005). As the inhibition of PI3K/Akt/mTOR is known to induce apoptosis, both AZ compounds showed severe apoptosis. In contrast, Rapamycin displayed minimal apoptosis. The enhanced ability of both AZ inhibitors to induce apoptosis may explain why both compounds showed higher activity against KF inhibition.

There is increasing evidence that the PI3K/Akt/mTOR network has an important role in ECM regulation in fibrosis (Ong *et al.*, 2007; Dazert and Hall, 2011). Collagen, FN, and α-SMA are proteins characteristic of the keloid phenotype (Ong *et al.*, 2007; Shih *et al.*, 2010). Overall, these proteins were selected to assess the effects on ECM production in response to both AZ compounds in KD. Both KU-0063794 and KU-0068650 reduced collagen I, FN, and α-SMA expression *in vitro* more significantly compared with Rapamycin.

We further explored the antitumour activity of both KU-0063794 and KU-0068650 in an *ex vivo* model (Bagabir *et al.*, 2012). Treating the keloid OC with both inhibitors demonstrated histologically reduced cellularity, inflammation, reduced hyalinized collagen bundles, and reduced the average keloid volume in a shrinkage assay. The effect of both compounds on PI3K/Akt/mTOR signaling and angiogenesis showed a significant reduction in p-mTOR and pAkt-S473 levels and significant anti-angiogenic properties. Analysis of the effect of both KU-0063794 and KU-0068650 on keloid-associated fibrotic markers showed strong inhibition of collagen I, FN, and α-SMA compared with Rapamycin, at low concentrations in an *ex vivo* model.

KU-0063794 is a potent and highly specific mTOR inhibitor for both mTORC1 and mTORC2, with an IC50 of 10 nM, but it does not suppress the activity of 76 other protein kinases or seven lipid kinases, including Class 1 PI3Ks at 1,000-fold higher concentrations (Garcia-Martinez *et al.*, 2009). In addition, there is no literature available on the efficacy of KU-0068650, which is similar in structure to both KU-0063794 and AZD8055. Moreover, the active form of mTOR (phospho-mTOR) is overexpressed in KD but not in normal skin (Ong *et al.*, 2007; Syed *et al.*, 2012a).

Overall, both AZ compounds show significant inhibition of primary KFs at very low concentrations. Indeed, a significant effect by both AZ compounds was only seen in primary normal skin fibroblasts at much higher concentrations, which could have resulted in nonspecific effects on these cells. Thus, the specificity of both AZ compounds is hitherto implied, as both seem to act selectively on cells with active levels of mTOR signaling.

Clinically adverse events have been demonstrated with the use of mTORC1 inhibitor, Sirolimus, and its analogs (Xue *et al.*, 2008; Lewis *et al.*, 2009; Jorge and David, 2011). However, AZD8055 (a similar compound structurally to both the AZ compounds used in this study) significantly reduced the clonogenic growth of leukemic progenitors from primary CD34 + Ve AML cells *ex vivo*. In contrast, exposure to AZD8055 barely affected the clonogenic growth of normal CD34 + Ve hematopoietic progenitors even at maximal concentrations (Willems *et al.*, 2012). As both AZ compounds are from a similar family of compounds to AZD8055, it is therefore plausible that both of these compounds may not be toxic to normal cells. However, this assertion remains to be formally tested in both of these AZ compounds. Importantly, it remains to be determined whether these compounds have a real measurable clinical effect on disease tissue in an *in vivo* scenario before their safe potential use in keloid patients.

Here, we propose a model for the mechanism of action of these compounds on KD (Supplementary Figure S10 online). The PI3K/Akt/mTOR axis is an important target in keloid pathogenesis, as dual inhibition of mTOR kinases by both the AZ compounds inhibits cell proliferation, migration, and invasion, and causes severe apoptosis compared with an allosteric mTORC1 inhibitor. Thus, both KU-0063794 and KU-0068650 dual mTORC1 and mTORC2 inhibitors may prove to be innovative therapeutic candidates for the treatment of keloid. Interestingly, both compounds showed higher efficacy in keloid compared with non-keloid derived cells. This could be due to active PI3K/Akt/mTOR axis in KF compared with ELFs, suggesting that both compounds are highly selective for PI3K/Akt/mTOR. Another important observation was that KU-0068650 showed a greater efficacy when compared with KU-0063794 at a similar concentration ($2.5\,\mu mol\,l^{-1}$) in every assay, possibly because of higher solubility, the presence of methyl groups, and lower IC50 of KU-0068650 (Supplementary Table S2 online).

MATERIALS AND METHODS
Patient selection and recruitment
This study was conducted in accordance with the ethical principles of Good Clinical Practice and the Declaration of Helsinki. This study received ethical approval from the local research committee (Manchester, UK), and all subjects gave full written, informed

consent. Keloid tissues were harvested at the time of surgery from patients confirmed to have clinical and pathological evidence of KD (Syed *et al.*, 2011; Bagabir *et al.*, 2012) (Supplementary Figure S1c online). Thirty-one keloid samples (out of 31 KD samples, 10 samples were used for *ex vivo* study) (Supplementary Table S1 online) were ethically consented (ethical approval was obtained from NHS Ethical Committee).

Establishment of primary fibroblast cultures

Keloid and ELTs (Supplementary Figure S1c online) (ELT samples were collected away from the keloid and importantly show no lesional involvement in hematoxylin and eosin) were collected in DMEM using a standard protocol to extract fibroblasts (Syed *et al.*, 2011, 2012a; Syed and Bayat, 2012a). In this study, passage 1 (p1) to passage 4 (p4) cells were used.

KU-0063794, KU-0068650, rapamycin, and campothecin compound regime

KU-0063794 and KU-0068650 (AstraZeneca, London, UK) (Supplementary Table S2 online) (2.5; 10; 15; 20 μmol l^{-1}) were compared with Rapamycin (Merck, Middlesex, UK) (5; 20 μmol l^{-1}). Camptothecin (Sigma-Aldrich, Dorset, UK) at a concentration of 250 ng ml^{-1} was used as positive control for RTCA, lactate dehydrogenase, WST-1, and apoptotic assays.

High-throughput In-Cell Western Blotting and quantification

Fibroblasts were treated with various concentrations of KU-0063794, KU-0068650, and Rapamycin, and In-Cell Western Blotting was performed using an optimized protocol (Syed and Bayat, 2012a; Syed *et al.*, 2012a,b). For all antibodies used, see Supplementary Tables S3 and S4 online.

Immunoprecipitation and fluorescent western blotting

Primary KFs (2.5×10^5 cells per well) were grown in 24-well plates for 24 hours. Cells were treated with compounds for 16 hours, and then lysed with cell lysis buffer ($1 \times$ radioimmunoprecipitation assay buffer, Cell Signaling, Hertfordshire, UK). mTOR (1:75) antibody was added and immune complexes were allowed to form by incubating on a rotor overnight at 4 °C. A ~50–55% slurry of protein G-Sepharose (Sigma-Aldrich) was added and incubation was carried out for 3 hours at 4 °C. Immunoprecipitates were captured with protein G-Sepharose, washed three times with cell lysis buffer, and analyzed by immunoblotting. Protein concentrations were determined using the bicinchoninic acid protein assay reagent kit (Thermo Scientific, Loughborough, UK). Equal amounts of protein (100 μg per Lane) were separated by NuPAGE Novex Bis-Tris Gels and transferred onto nitrocellulose membranes using iBlot Dry blotting device (Invitrogen, Paisley, UK). Membranes were blocked with blocking buffer (LI-COR, Cambridge, UK) for 30–45 minutes at room temperature. The membranes were incubated with different concentrations of primary antibodies (Supplementary Table S3 online) overnight at 4 °C. After incubation, the membranes were washed and incubated with secondary antibodies (Supplementary Table S4 online) for 1 hour 15 minutes at room temperature. The membranes were washed and the signal was detected using the Odyssey infrared imaging system (LI-COR); β-actin served as loading control.

Label-free RTCA to determine the effect of different concentrations of the compounds

We used a label-free RTCA on a microelectronic system to measure cell attachment, spreading, and proliferation. The basic principle of the RTCA system and the optimized protocol were described previously in detailed (Xing *et al.*, 2005; Syed and Bayat, 2012a; Syed *et al.*, 2012b).

In vitro two-dimensional migration assay

The assay was performed as described previously (Syed *et al.*, 2012a; Syed and Bayat, 2012b). Briefly, a Oris 96-well plate (Oris migration assay kit, Cambridge Bioscience, Cambridge, UK) was coated with 9 μg ml^{-1} rat-tail collagen (BD Bioscience, Oxford, UK) and incubated for 30–45 minutes at 37 °C/5% CO_2. After incubation, Oris cell seeding stoppers were inserted according to the manufacturer's instructions. Serum-starved KFs and ELFs were pre-labeled with PKH26 (Sigma-Aldrich) according to the manufacturer's instructions. A density of 2.5×10^5 cells per well was seeded in each well of the Oris 96-well migration assay plates. The plate was then incubated overnight at 37 °C/5% CO_2. The next day, the cell seeding stoppers were removed and 100 μl of fresh medium was added with or without different compounds as above; the plates were further incubated and the cells were allowed to migrate for ~30 hours in the migration zone. Micrographs were captured using × 4 magnification of inverted microscopy (Olympus UK, Southend-on-Sea, UK). Cells in the migration zone were counted from four independent experiments and average migrated cells were plotted on the graphs.

In vitro three-dimensional invasion assay

Inhibition of the invasive capacity of KU-0063794, KU-0068650, and Rapamycin was tested using basement membrane extract *in vitro* in three-dimensional invasion assay (Oris Invasion and detection assay kit, Cambridge Bioscience) as described previously (Syed and Bayat, 2012a; Syed *et al.*, 2012a). Briefly, serum-starved cells at a density of 2.5×10^5 cells per well were seeded in Oris invasion assay plates and allowed to attach for 8–12 hours at 37 °C/5% CO_2; after cell attachment, the stoppers were removed from the wells and cells were washed once with phosphate-buffered saline and 40 μl of basement membrane extract was added to the cells. The plates were incubated (at 37 °C, 5% CO_2) for 45–60 minutes. Compound treatments were given for 48 hours and cells were allowed to invade in the 2-mm invasion zone created by Oris cell seeding stoppers. The cells were stained with Calcein AM according to the manufacturer's instructions. Micrographs were captured using × 4 magnification of inverted Olympus IX71 (Olympus UK Ltd., Southend-on-Sea, UK) microscopy. Invaded cells in the invasion zone were counted from four independent experiments and average invaded cells were plotted on the graphs.

Please see Supplementary data online for methodology used in this study.

group do not hold any intellectual property or rights to the use or sale of these particular compounds as they remain the sole property of AZ.

SUPPLEMENTARY MATERIAL

Supplementary material is linked to the online version of the paper at http://www.nature.com/jid

REFERENCES

Bagabir R, Syed F, Paus R *et al.* (2012) Long-term organ culture of keloid disease tissue. *Exp Dermatol* 21:376–81

Benjamin D, Colombi M, Moroni C *et al.* (2011) Rapamycin passes the torch: a new generation of mTOR inhibitors. *Nat Rev Drug Discov* 10:868–80

Bracho-Valdes I, Moreno-Alvarez P, Valencia-Martienz I *et al.* (2011) mTORC1-and mTORC2-interacting proteins keep their multifunctional partners focused. *IUBMB Life* 63:896–914

Chapuis N, Tamburini J, Green AS *et al.* (2010) Dual inhibition of PI3K and mTORC1/2 signaling by NVP-BEZ235 as a new therapeutic strategy for acute myeloid leukemia. *Clin Cancer Res* 16:5424–35

Chresta CM, Davies BR, Hickson I *et al.* (2010) AZD8055 is a potent, selective, and orally bioavailable ATP-competitive mammalian target of rapamycin kinase inhibitor with *in vitro* and *in vivo* antitumor activity. *Cancer Res* 70:288–98

Dazert E, Hall MN (2011) mTOR signaling in disease. *Curr Opin Cell Biol* 23:744–55

Dormond-Meuwly A, Roulin D, Dufour M *et al.* (2011) The inhibition of MAPK potentiates the anti-angiogenic efficacy of mTOR inhibitors. *Biochem Biophys Res Commun* 407:714–9

Garcia-Martinez JM, Moran J, Clarke RG *et al.* (2009) Ku-0063794 is a specific inhibitor of the mammalian target of rapamycin (mTOR). *Biochem J* 421:29–42

Jacinto E, Loewith R, Schmidt A *et al.* (2004) Mammalian TOR complex 2 controls the actin cytoskeleton and is rapamycin insensitive. *Nat Cell Biol* 6:1122–8

Janes MR, Limon JJ, So L *et al.* (2010) Effective and selective targeting of leukemia cells using a TORC1/2 kinase inhibitor. *Nat Med* 16:205–13

Jorge LJ, David S (2011) Potential therapeutic roles for inhibition of the PI3K/Akt/mTOR pathway in the pathophysiology of diabetic retinopathy. *J Ophthalmol* 2011. doi:10.1155/2011/589813

Lewis GP, Chapin EA, Byun J *et al.* (2009) Muller cell reactivity and photoreceptor cell death are reduced after experimental retinal detachment using an inhibitor of the Akt/mTOR pathway. *Invest Ophthalmol Vis Sci* 50:4429–35

Lim IJ, Phan TT, Tan EK *et al.* (2003) Synchronous activation of ERK and phosphatidylinositol 3-kinase pathways is required for collagen and extracellular matrix production in keloids. *J Biol Chem* 278:40851–8

Malagu K, Duggan H, Menear K *et al.* (2009) The discovery and optimisation of pyrido [2, 3-d] pyrimidine-2, 4-diamines as potent and selective inhibitors of mTOR kinase. *Bioorg Med Chem Lett* 19:5950–3

Mall JW, Pollmann C, Muller JM *et al.* (2002) [Keloid of the earlobe after ear piercing. Not only a surgical problem]. *Chirurg* 73:514–6

Marshall G, Howard Z, Dry J *et al.* (2011) Benefits of mTOR kinase targeting in oncology: pre-clinical evidence with AZD8055. *Biochem Soc Trans* 39:456–9

Morgensztern D, McLeod HL (2005) PI3K/Akt/mTOR pathway as a target for cancer therapy. *Anticancer Drugs* 16:797–803

Ong CT, Khoo YT, Mukhopadhyay A *et al.* (2007) mTOR as a potential therapeutic target for treatment of keloids and excessive scars. *Exp Dermatol* 16:394–404

Patel NP, Lawrence Cervino A (2010) Keloid treatment: is there a role for acellular human dermis (Alloderm)? *J Plast Reconstr Aesthet Surg* 63:1344–8

Santiskulvong C, Konecny GE, Fekete M *et al.* (2011) Dual targeting of phosphoinositide 3-kinase and mammalian target of rapamycin using NVP-BEZ235 as a novel therapeutic approach in human ovarian carcinoma. *Clin Cancer Res* 17:2373–84

Shegogue D, Trojanowska M (2004) Mammalian target of rapamycin positively regulates collagen type I production via a phosphatidylinositol 3-kinase-independent pathway. *J Biol Chem* 279:23166–75

Shih B, Garside E, McGrouther DA *et al.* (2010) Molecular dissection of abnormal wound healing processes resulting in keloid disease. *Wound Repair Regen* 18:139–53

Sini P, James D, Chresta C *et al.* (2010) Simultaneous inhibition of mTORC1 and mTORC2 by mTOR kinase inhibitor AZD8055 induces autophagy and cell death in cancer cells. *Autophagy* 6:553–4

Sparks CA, Guertin DA (2010) Targeting mTOR: prospects for mTOR complex 2 inhibitors in cancer therapy. *Oncogene* 29:3733–44

Syed F, Ahmadi E, Iqbal SA *et al.* (2011) Fibroblasts from the growing margin of keloid scars produce higher levels of collagen I and III compared with intralesional and extralesional sites: clinical implications for lesional site-directed therapy. *Br J Dermatol* 164:83–96

Syed F, Bayat A (2012a) Notch signalling pathway in keloid disease: Enhanced fibroblast activity in a Jagged-1 peptide dependent manner in lesional versus extra-lesional fibroblasts. *Wound Repair Regen* 20: 688–706

Syed F, Bayat A (2012b) Superior effect of combination versus single steroid therapy in keloid disease: a comparative *in vitro* analysis of glucocorticoids. *Wound Repair Regen* doi:10.1111/j.1524-475X.2012. 00862.x

Syed F, Sherris D, Paus R *et al.* (2012a) Keloid disease can be inhibited by antagonizing excessive mTOR signalling with a novel dual TORC1/2 inhibitor. *Am J Pathol* 181:1642–58

Syed F, Thomas A, Singh S *et al.* (2012b) *In vitro* study of novel collagenase (Xiaflex®) on Dupuytren's disease fibroblasts displays unique drug related properties. *PloS One* 7:e31430

Vincent AS, Phan TT, Mukhopadhyay A *et al.* (2007) Human skin keloid fibroblasts display bioenergetics of cancer cells. *J Invest Dermatol* 128:702–9

Willems L, Chapuis N, Puissant A *et al.* (2012) The dual mTORC1 and mTORC2 inhibitor AZD8055 has anti-tumor activity in acute myeloid leukemia. *Leukemia* 26:1195–202

Xing JZ, Zhu L, Jackson JA *et al.* (2005) Dynamic monitoring of cytotoxicity on microelectronic sensors. *Chem Res Toxicol* 18:154–61

Xue Q, Hopkins B, Perruzzi C *et al.* (2008) Palomid 529, a novel small-molecule drug, is a TORC1/TORC2 inhibitor that reduces tumor growth, tumor angiogenesis, and vascular permeability. *Cancer Res* 68:9551

Yu K, Shi C, Toral-Barza L *et al.* (2010) Beyond rapalog therapy: preclinical pharmacology and antitumor activity of WYE-125132, an ATP-competitive and specific inhibitor of mTORC1 and mTORC2. *Cancer Res* 70:621

Zhang Q, Kelly AP, Wang L *et al.* (2006) Green tea extract and (−)-epigallocatechin-3-gallate inhibit mast cell-stimulated type I collagen expression in keloid fibroblasts via blocking PI-3K/Akt signaling pathways. *J Invest Dermatol* 126:2607–13